Photonic bandgaps and resonators in the one-stage Sierpinski gasket basis

D. W. Cooley[1,*] and David R. Andersen[2]

[1]Department of Electrical and Computer Engineering, The University of Iowa, Iowa City, Iowa 52242, USA
[2]Department of Electrical and Computer Engineering and Department of Physics and Astronomy, The University of Iowa, Iowa City, Iowa 52242, USA
*Corresponding author: cooley@ostc.physics.uiowa.edu

Received January 26, 2007; revised May 9, 2007; accepted May 18, 2007; posted May 24, 2007 (Doc. ID 79359); published August 14, 2007

This paper discusses theoretical calculations of photonic bandgaps found in the one-stage Sierpinski gasket basis in the hexagonal lattice. Dielectric triangles and cylinders as well as air triangles and cylinders are investigated. All of these structures exhibited complete bandgaps, with the largest complete gap having 6.1% fractional width. The largest TE and TM polarization gaps were 23% and 40% fractional width, respectively. Resonators constructed from these crystals with a Q ten to 2000 times greater than resonators constructed using one cylinder in the hex lattice are demonstrated. © 2007 Optical Society of America

OCIS codes: 230.5750, 230.3990.

1. INTRODUCTION

Yablonovitch [1] and John [2] introduced photonic crystals—the idea that a dielectric material could possess bandgaps, or regions of frequency in which propagation of light waves is prohibited by Bragg reflection. Interest in photonic crystals has increased over time, and several review articles are available in the literature [3,4]. Application areas for photonic crystals are increasing rapidly, including photonic crystal fibers, photonic crystal lasers, and waveguides. A considerable amount of research has been done on the existence of bandgaps for various basis shapes and lattices [5–7]. One rule of thumb for the existence of bandgaps in photonic crystals is that TE polarization gaps are favored by dielectric structures comprised of interconnected dielectric regions, and TM polarization gaps are favored in crystals with disconnected regions of high dielectric constant [8]. Research on bandgaps in photonic crystals is also being done on fractal or self-similar structures. Li *et al.* [9] presented research on complete bandgaps in two-dimensional fractal photonic crystal structures comprised of dielectric cylinders in air or air cylinders in a dielectric. Sakoda *et al.* [10] investigated the Menger sponge fractal using finite-difference time-domain (FDTD) methods. Liu *et al.* [11] studied crystals with a basis formed by two n-stage Sierpinski gaskets in the hexagonal lattice. The Sierpinski crystal basis studied here is different than those in Ref. [11], which consist of two Sierpinski gaskets constructed inside equilateral triangles and combined into a rhombus. The crystals used here have only one gasket inside a triangle, with the remainder of the basis formed of air or dielectric. Also in this work we consider crystals formed by replacing the triangular features with cylinders, because they would be easier to fabricate.

Resonators can be constructed inside photonic crystals by creating defects in a crystal lattice [12]. The resonant frequency of the resonator can be tuned by adjusting the defect size. The resonator Q increases with the size of the crystal around the defect. These resonators are used in drop filters [13,14] and all pass filters [15], for example. References [13,15] discuss filters using one dielectric cylinder in the square lattice, while Ref. [14] discusses a drop filter using one air cylinder in the hexagonal lattice. The Q of the drop filter determines the channel capacity of the device—a filter with a higher Q will have a greater channel capacity.

This paper covers theoretical calculations on the existence of photonic bandgaps in the two-dimensional one-stage Sierpinski gasket and resonators constructed using this crystal. To construct the Sierpinski gasket, one begins with an equilateral triangle, as shown in Fig. 1(a). The points that bisect each side of the triangle form a smaller triangle, which is removed from the initial shape, resulting in the one-stage Sierpinski gasket, Fig. 1(b). This process is then repeated on each of the three triangles, creating the two-stage Sierpinski gasket, as in Fig. 1(c), etc. The one-stage Sierpinski gasket with three triangles in the hexagonal basis as shown in Fig. 1(d) is studied in this paper because it contains interconnected regions of dielectric that are somewhat isolated and thus may exhibit complete gaps. One of the gaskets is then placed in the hexagonal lattice. The basis obtained by replacing the triangles with circles of equal area is also investigated, because fabrication of photonic crystals with features of circular cross section is easier than fabrication of triangular features. Since TE gaps are supported by connected dielectric regions and the basis with circular features has less connectivity, it is expected that the TE gaps will be inhibited in the basis with circular features. The inverse structures consisting of air triangles and air cylinders in a dielectric are also studied in this paper.

These simple fractal crystals are studied because they possess complete gaps as well as large TE/TM polarization gaps, as discussed below. Since complete gaps are

0740-3224/07/100A84-5/$15.00 © 2007 Optical Society of America

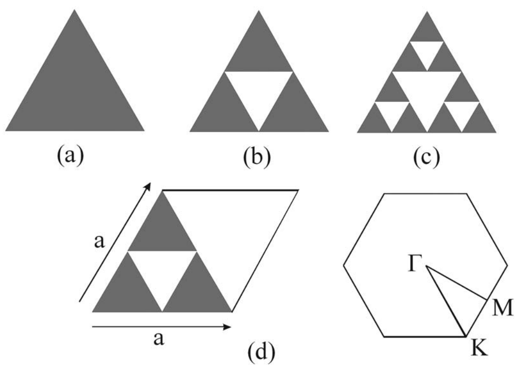

Fig. 1. (a)–(c) Construction of Sierpinski gasket. (d) Three triangle basis and Brillouin zone for hexagonal lattice.

present the system designer could use any polarization of light desired with these crystals instead of TE or TM polarization only. Another reason for study of this structure is that resonators constructed with these crystals have a much higher Q than is present using either one dielectric cylinder in the square lattice or one air cylinder in the hex lattice, as discussed in Section 2. This will lead to higher channel capacity when used in wave division multiplexing (WDM) networks.

In the remainder of this paper results from calculating gap maps for the four basis shapes described above will be summarized. The Q of resonators constructed with these crystals will be compared to that of resonators constructed with one air cylinder in the hexagonal lattice and one dielectric cylinder in the square lattice.

2. RESULTS AND DISCUSSION

The method of calculating the band structures starts with Faraday's law,

$$\nabla \times \vec{E} = -\frac{1}{c}\frac{\partial \vec{B}}{\partial t}, \qquad (1)$$

and Ampere's law,

$$\nabla \times \vec{H} = \frac{1}{c}\frac{\partial \vec{D}}{\partial t}, \qquad (2)$$

in cgs units. In dielectric materials we may set $B=H$ and for fields of the form $\vec{E}(r,t)=\vec{E}(r)e^{i\omega t}$ and $\vec{H}(r,t)=\vec{H}(r)e^{i\omega t}$, we have

$$\nabla \times \vec{E}(r) = -\frac{i\omega}{c}\vec{H}(r), \qquad (3)$$

$$\nabla \times \vec{H}(r) = \frac{i\omega}{c}\epsilon(r)\vec{E}(r). \qquad (4)$$

Dividing Eq. (4) by the dielectric constant, taking the curl of both sides, and substituting Eq. (3) results in an eigenvalue problem for the magnetic field,

$$\nabla \times \left(\frac{1}{\epsilon}\nabla \times \vec{H}(r)\right) = \left(\frac{\omega}{c}\right)^2 \vec{H}(r). \qquad (5)$$

We seek solutions to Eq. (5) at points on the edge of the Brillouin zone of the hexagonal lattice. Fully vectorial eigenmodes of Eq. (5) with periodic boundary conditions were computed by a preconditioned conjugate-gradient minimization of the block Rayleigh quotient in a plane-wave basis [16]. The resolution used in computations was sufficiently high that mode frequencies had converged to within 1%. Band structures for the one-stage Sierpinski gasket basis in the hexagonal lattice have been computed for a range of values of dielectric constant. The area-filling fraction of triangles was also varied by varying the size of triangles but keeping the location of the center of the triangle constant. Dielectric triangles in air and air triangles in a dielectric were studied, as well as air and dielectric cylinders.

The largest TE, TM, and complete bandgap sizes are summarized in Table 1. Figure 2 shows the band structure for the crystal with the largest complete gap of width 6.1% and the three dielectric triangle basis with dielectric constant of 12. The dielectric constant used for the gap maps versus the filling fraction is 12. The area of the cylinders for the gap maps versus the dielectric constant is equal to that of the three triangle basis with triangles just touching. Dielectric constants of 4–14 were considered. All four of the basis shapes exhibited a complete gap. Large TE and TM polarization gaps of 23% and 40% width, respectively, were found in the three cylinder basis. A comparison of the gap maps for all considered crystals showed that the number of TE gaps that occur in the three cylinder basis is reduced compared to the three triangle crystals as expected. However, the largest TE polarization gap was found in the three-cylinder basis.

To attempt to gain insight into the formation of bandgaps in these crystals the amount of electric energy in the dielectric for the dielectric and air bands below and above the complete gaps was analyzed. Table 2 shows a summary of the electric energy in the dielectric and air bands for the crystals studied. We have considered the K and M points of the Brillouin zone. For the lowest band the high D field will be located in regions of high dielectric constant, because the fields minimize the energy functional [17],

Table 1. TE, TM, and Complete Bandgaps for Each of the Four Basis Types Considered[a]

Basis	Gap Type	ϵ	Filling Fraction	Gap Size (%)
3 Triangle	TE	12	0.25	10.7
3 Triangle	TM	12	0.16	37.2
3 Triangle	Complete	12	0.14	6.1
3 Cylinder	TE	12	0.68	23.1
3 Cylinder	TM	12	0.16	40.1
3 Cylinder	Complete	12	0.48	2.7
3 Air Tri.	TE	12	0.36	8.8
3 Air Tri.	TM	14	0.63	5.0
3 Air Tri.	Complete	5.8	0.63	2.3
3 Air Cyl.	TE	12	0.55	18.2
3 Air Cyl.	TM	12	0.68	30.7
3 Air Cyl.	Complete	12	0.65	5.0

[a]The largest gaps from gap maps versus epsilon and filling fraction are shown.

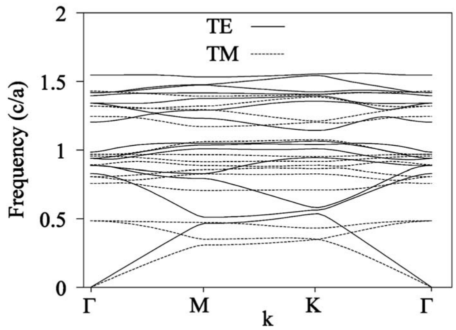

Fig. 2. Band structure of three triangle basis with largest complete gap. Fractional area is 0.14. Complete gap of 6.1% is just above a frequency of 1.

$$E_f(\vec{H}) = \left(\frac{1}{2(\vec{H},\vec{H})}\right) \int d\vec{r} \frac{1}{\epsilon} \left| \frac{\omega}{c} \vec{D} \right|^2 . \tag{6}$$

The higher bands will seek to minimize the energy functional while being orthogonal to the lower bands. The high D field regions will be in regions with high dielectric constant. This leads to the dielectric band having higher D field energy in the dielectric than the air band for low enough frequencies. Table 2 shows that there is no simple relationship between the electric energy in the dielectric for the dielectric and air bands. Looking at the dielectric and air-band field structures for the three triangle basis shown in Fig. 3, we see that the field structures are fairly complicated, with the air band forming a circular node within the dielectric material. It appears that the frequency is high enough that for the three triangle basis the field structure is complicated enough to allow more D field energy in the air band than in the dielectric band. Thus for the basis types studied the field structures are quite complicated, and we did not discover a clear relationship between dielectric and air band energies.

To verify the modeling results for the hexagonal basis a gap map for one dielectric cylinder in the hexagonal lattice was constructed. Figure 4 shows the gap map versus filling fraction for a dielectric constant of 12 in the hexagonal lattice. This gap map compares well with previous results for the hexagonal lattice [18,19].

The existence of bandgaps in the two-stage Sierpinski gasket with nine triangles was also briefly investigated. The TE and TM polarization gaps found in the nine triangle structures studied were smaller in fractional width than gaps in the three triangle structure, and no complete gaps were noted. In Ref. [11] it is also noted that as the stage of the fractal increases the band structure compresses in frequency, reducing or eliminating bandgaps as the structure becomes more complex.

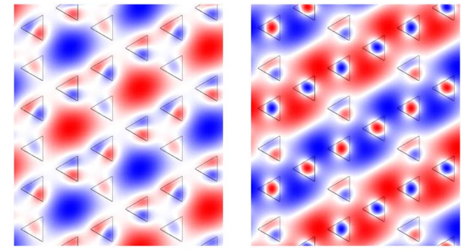

Fig. 3. (Color online) (a) Dielectric and (b) air bands for TM polarization at M point. Z component of the E field is shown.

To investigate resonators with the Sierpinski gasket basis crystals we utilize the FDTD method [20,21] with perfectly matched layers [22] around the outside of the computation area to absorb any stray fields. We simulated resonators using the crystal from Table 1 with the largest TE or TM polarization bandgap. Table 1 shows that the largest gap of 40.1% was obtained for the TM polarization in the three dielectric cylinder basis with a filling fraction of $0.16a$, corresponding to a cylinder radius of $0.12a$. For comparison we also simulated resonators using one air cylinder in the hexagonal lattice using the geometry from Ref. [14]. There air holes in a dielectric were used since out of plane losses are avoided with that type of structure and for other fabrication advantages.

The Q of resonators of various sizes were calculated by exciting a Gaussian field at a point source inside the resonator and measuring the decay rate of the fields inside the resonator after the fields were turned off. Since energy in the resonator decays proportional to $\exp(-\omega_0 t/Q)$, the Q is estimated as

$$Q = -\frac{\omega_0(N_1 - N_0)\Delta t}{2\ln(H_1/H_0)}, \tag{7}$$

[23] where H_0 and H_1 are the field amplitudes at time steps N_0 and N_1. As shown in Fig. 5, the resonator modes for the three-cylinder basis crystal are nondegenerate

Table 2. Fraction of D Field Energy in Dielectric and Air Bands, with Indication Whether the Dielectric Band Energy is Greater or Less Then the Air Band Energy

		TE bands			TM bands		
Basis	k point	Dielectric	>or<	Air	Dielectric	>or<	Air
3 Triangle	K	0.536	>	0.193	0.561	<	0.640
3 Triangle	M	0.810	>	0.259	0.571	<	0.612
3 Cylinder	K	0.379	<	0.505	0.912	>	0.911
3 Cylinder	M	0.376	<	0.431	0.973	>	0.888
3 Air Tri.	K	0.806	>	0.755	0.979	>	0.946
3 Air Tri.	M	0.872	>	0.745	0.959	>	0.943
3 Air Cyl.	K	0.764	<	0.925	0.928	<	0.962
3 Air Cyl.	M	0.850	<	0.920	0.949	<	0.952

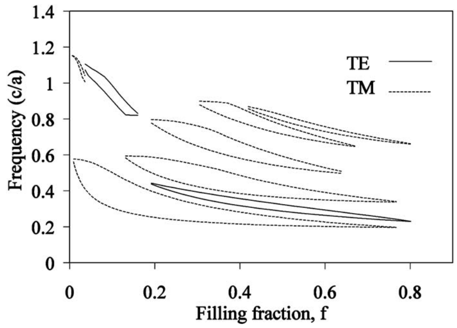

Fig. 4. Gap map versus filling fraction for one cylinder in hexagonal lattice with a dielectric constant of 12.

monopole modes. Figure 6 shows the Q values for the three dielectric cylinder Sierpinski basis and one air cylinder basis crystals. The result is that three cylinder Sierpinski crystals have a Q approximately 10, 100, 300, and 2000 times greater than one air cylinder crystals for crystals with 1, 2, 3, and 4 rows of basis cells around the resonator. This is due to the relatively smaller size of the resonator formed in the three cylinder basis by removing one cylinder. Resonators confined by more rows of basis cells have higher Q, so it is reasonable to expect that the Q will increase if the resonator is made smaller. These high-Q resonators may then be used in structures such as channel-drop filters in WDM networks to increase channel capacity. Also, the Q values for one dielectric cylinder in a square lattice from Ref. [12] are three to five times the Q for one air cylinder in the hex lattice shown in Fig. 6, so the three-cylinder Sierpinski crystal would still have considerably higher Q than for one dielectric cylinder in the square lattice.

3. SUMMARY

Complete bandgaps are present in the three dielectric triangle and cylinder bases as well as the air triangle and air cylinder bases in the hexagonal lattice. The largest complete gap was found in the three triangle basis, and the largest TE and TM gaps were in the three cylinder basis. The TE polarization gaps were inhibited in the three cylinder basis relative to the three triangle basis owing to the rule of thumb for TE gaps being favored in a connected dielectric crystal. Resonators constructed from the three dielectric cylinder basis in the hexagonal lattice have considerably higher Q than resonators constructed using one air cylinder in the hex lattice or one dielectric cylinder in the square lattice. The increased resonator Q may lead to channel drop filters and WDM networks with increased channel capacity.

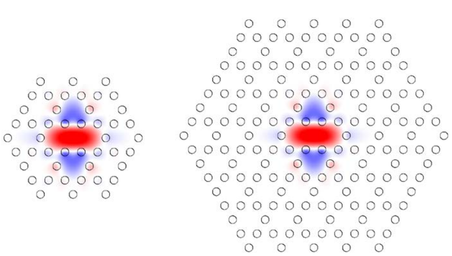

(a) (b)

Fig. 5. (Color online) Resonator modes for three dielectric cylinders in hex lattice with (a) two and (b) four rows of the crystal basis around the resonator.

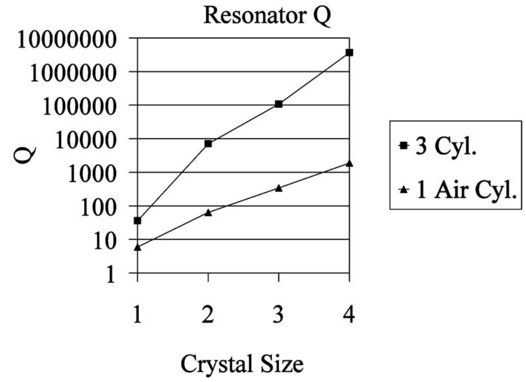

Fig. 6. Resonator Q versus the number of crystal basis cells around resonator for three dielectric cylinder Sierpinski basis and three air cylinders. Both are in hexagonal lattice.

ACKNOWLEDGMENTS

D.R.A. acknowledges support from the National Science Foundation and the National Institutes of Health.

REFERENCES

1. E. Yablonovitch, "Inhibited spontaneous emission in solid-state physics and electronics," Phys. Rev. Lett. **58**, 2059–2062 (1987).
2. S. John, "Strong localization of photons in certain disordered dielectric superlattices," Phys. Rev. Lett. **58**, 2486–2489 (1987).
3. J. D. Joannopoulos, P. R. Villeneuve, and S. Fan, "Photonic crystals: putting a new twist on light," Nature (London) **386**, 143–149 (1997).
4. C. Lopez, "Three-dimensional photonic bandgap materials: semiconductors for light," J. Opt. A **8**, R1–R14 (2006).
5. R. Wang, X. H. Wang, B. Y. Gu, and G. Z. Yang, "Effects of shapes and orientations of scatterers and lattice symmetries on the photonic band gap in two-dimensional photonic crystals," J. Appl. Phys. **90**, 4307–4313 (2001).
6. W. Kuang, Z. Hou, Y. Liu, and H. Li, "The bandgap of a photonic crystal with triangular dielectric rods in a honeycomb lattice," J. Opt. A, Pure Appl. Opt. **7**, 525–528 (2005).
7. N. Susa, "Large absolute and polarization-independent photonic band gaps for various lattice structures and rod shapes," J. Appl. Phys. **91**, 3501–3510 (2002).
8. R. D. Meade, A. M. Rappe, K. D. Brommer, and J. D. Joannopoulos, "Nature of the photonic band gap: some insights from a field analysis," J. Opt. Soc. Am. B **10**, 328–332 (1993).
9. L. Li, Y. C. Xie, Y. Q. Wang, X. Y. Hu, Z. F. Feng, and B. Y. Cheng, "Absolute gap of two-dimensional fractal photonic structure," Chin. Phys. Lett. **20**, 1767–1769 (2003).
10. K. Sakoda, S. Kirihara, Y. Miyamoto, M. W. Takeda, and K. Honda, "Light scattering and transmission spectra of the Menger sponge fractal," Appl. Phys. B: Photophys. Laser Chem. **81**, 321–324 (2005).
11. Z. Liu, J. J. Xu, and Z. F. Lin, "Photonic band gaps in two-dimensional crystals with fractal structure," Chin. Phys. Lett. **20**, 516–518 (2003).
12. P. R. Villeneuve, S. Fan, and J. D. Joannopoulos, "Microcavities in photonic crystals: mode symmetry, tunability, and coupling efficiency," Phys. Rev. B **54**, 7837–7842 (1996).

13. S. Fan, P. R. Villeneuve, J. D. Joannopoulos, and H. A. Haus, "Channel drop tunneling through localized states," Phys. Rev. Lett. **80**, 960–963 (1998).
14. M. Qiu and B. Jaskorzynska, "Design of a channel drop filter in a two-dimensional triangular photonic crystal," Appl. Phys. Lett. **83**, 1074–1076 (2003).
15. Z. Wang and S. Fan, "Compact all-pass filters in photonic crystals as the building block for high-capacity optical delay lines," Phys. Rev. E **68**, 066616(1)–(4) (2003).
16. S. G. Johnson and J. D. Joannopoulos, "Block-iterative frequency domain methods for Maxwell's equations in a planewave basis," Opt. Express **8**, 173–190 (2001).
17. J. D. Joannopoulos, R. D. Meade, and J. N. Winn, *Photonic Crystals* (Princeton U. Press, 1995).
18. J. N. Winn, R. D. Meade, and J. D. Joannopoulos, "Two-dimensional photonic band-gap materials," J. Mod. Opt. **41**, 257–273 (1994).
19. R. Padjen, J. M. Gerard, and J. Y. Marzin, "Analysis of the filling pattern dependence of the photonic bandgap for two-dimensional systems," J. Mod. Opt. **41**, 295–310 (1994).
20. A. Taflove and S. C. Hagness, *Computational Electrodynamics: the Finite Difference Time Domain Method*, 3rd Ed. (Artech House, 2005).
21. FDTD software is available at http://ab-initio.mit.edu/meep, for example.
22. J. P. Berenger, "A perfectly matched layer for the absorption of electromagnetic waves," J. Comput. Phys. **114**, 185–200 (1994).
23. S. Gao and S. Albin, "Numerical techniques for excitation and analysis of defect modes in photonic crystals," Opt. Express **11**, 1080 (2003).